Sovling NP Graph Problem with Quantum Z_2 Lattice Gauge Theory

Xiaopeng Cui[1] and Yu Shi[1, *]

[1] *Department of Physics & State Key Laboratory of Surface Physics,*

Fudan University, Shanghai 200433, China

Abstract

In this paper, using the condensed close string characteristics of Z_2 topological quantum phase transition, by mapping a graph to a lattice we develop a adiabatic quantum algorithm with time complexity $O(\frac{1}{g_c^2}\sqrt{\frac{1}{\varepsilon}N_e^{3/2}(N_v^3 + \frac{N_e}{g_c})})$ to obtain the closed string condensate of its corresponding lattice, which is helpful to solve the Hamilton cycle problem (HCP) of the graph. Using this algorithm model, by the simulation of a number of small random graphs we find that the number of Hamiltonian cycles in a graph has a significant effect on the critical parameter g_c of Z_2 topological quantum phase transition of its corresponding lattice, the mean value of g_c with $\sqrt{N_{hc}}$ (N_e, N_v is fixed) and the mean value of $\frac{1}{g_c}$ with N_e (N_v is fixed) are all a linear relationship. Based on this, we further discuss the possibility of a algorithm which uses g_c to infer the number of Hamiltonian cycles in a graph on a quantum computer.

---

* yushi@fudan.edu.cn

I. INTRODUTION

In the mathematical field of graph theory the Hamiltonian cycle problem(HCP) is a problem of determining whether a Hamiltonian cycle (a cycle in an undirected graph that visits each vertex exactly once) exists in a given undirected graph[1]. A undirected graph is made up of N_v vertices which are connected by N_e edges without directions. HCP is a famous NP problem and also a NP-complete(NPC) problem which means all other NP problems can reducible to HCP in polynomial time[2]. Therefore, the solution of HCP problem will greatly promote the solution of $P = NP$ problem. So far, the best algorithm to solve this problem in a classical computer is a dynamic programming algorithm(Bellman, Held, and Karp) in time complexity $O(N_v{}^2 2^{N_v})$[3] and a Monte Carlo algorithm in time complexity $O(1.657^{N_v})$[4]. With the development of quantum computer, the advantages of quantum algorithm gradually appear. Such as Shor's algorithm is a polynomial-time quantum computer algorithm for integer factorization which is a NP problem in classical computer[5]. Shor's algorithm greatly advanced the theory of computer science. But there is still no a quantum accelerated algorithm of polynomial time complexity for HCP[6]. So, $P = NP$ is also still a challenging problem on quantum computer. However, we find that Z_2 gauge theory and string-net theory provide new possibilities for this problem.

Lattice gauge theory is the study of gauge theories on a spacetime that has been discretized into a lattice. Z_2 gauge theory is the simplest lattice gauge theory and also a quantum spin model[7, 8], which can be reformulated as a closed string theory[9, 10]. For Z_2 lattice gauge theory, there are two different phases which are separated by a TQPT as the parameter g changes. These two phases are deconfined phase and confined phase. In the deconfined phase, the ground state of the lattice system is a closed string condenstate[10]. In the closed string condenstate, all configurations of qubits in the lattice are closed string configurations, and the closed strings passing through all regions are Hamiltonian cycles. Therefore, the closed string condenstate can be prepared by TQPT induced by adiabatic change of g and then we can find Hamiltonian cycles more easily by some quantum search algorithms in this condensed state.

Because any graph can be mapped to a lattice, this method for finding Hamiltonian cycles can be generalized to any graph. In addition, the number of Hamiltonian cycles in the graph may have an impact on the TQPT critical parameter g_c, which has the potential

to provide a new solution of lower time complexity for HCP, thus providing a new possibility for P=NP problem on quantum computer. In addition, owing to the important position of graph theory in computer science and mathematics, for example, deep learning represented by deep neural networks are being integrated with graphical models[11, 12]. This quantum model of graph problems will also benefit the development of these research[13, 14].

The key to the above scheme is using quantum simulation of adiabatic evolution to induce the TQPT of the lattice on a quantum computer. With the development of quantum computer, quantum simulation have become a new powerful research tool for studying the TQPT of Z_2 gauge theory[15–18]. This paper uses the digital quantum adiabatic simulation method[19–21] based on quantum circuit model[17] to gradually change g to get the closed string condenstate.

II. CLOSED STRING AND HAMILTONIAN CYCLE OF Z_2 DECONFINED PHASE IN A TORUS LATTICE

The Hamiltonian of the quantum Z_2 gauge theory[8, 17, 22] is defined as

$$H = Z + gX \tag{1}$$

$$X = -\sum_l \sigma_l^x, \ Z = \sum_\square Z_\square, \ Z_\square = -\prod_{l \in \square} \sigma_l^z \tag{2}$$

where the $\square$ indicates the elementary plaquette of the lattice.

For 3×3 tours lattice, the boundary conditions are shown in the Fig.1(a). When g is relatively small, the ground state of the system is in deconfined phase; when g is relatively large, the ground state of the system is in confined phase. During this period, a TQPT is experienced, and the critical parameter of phase transition is g_c.

At $g = 0$, the starting ground state is $|\psi_0\rangle$. The starting ground state $|\psi_0\rangle$ is $Z_\square = -1, \forall \square$ and $Z = -9$. In the $M * N$ torus lattice with $N_v = M \times N$ plaquettes, $|\psi_0\rangle = \sum_{i=1}^{S_0} |\phi_i\rangle$ contains $S_0 = 2^{N_e}/(2^{N_v-1})$ superposed base vector components $|\phi_i\rangle$, and $Z = -9$ for every $|\phi_i\rangle$. $N_e = 2N_v$ is the link or edge number of the tours lattice. In the lattice, a cycle through the edges in $|0\rangle$ state forms a closed string[9]. This starting ground state is also a closed string condensed state, each $|\phi_i\rangle$ corresponds to a kind of closed string configurations[9]. So there are a total of S_0 closed string configurations in the starting ground state. Two of these configurations are shown in the Fig.2. In the configuration of Fig.2(a), a single
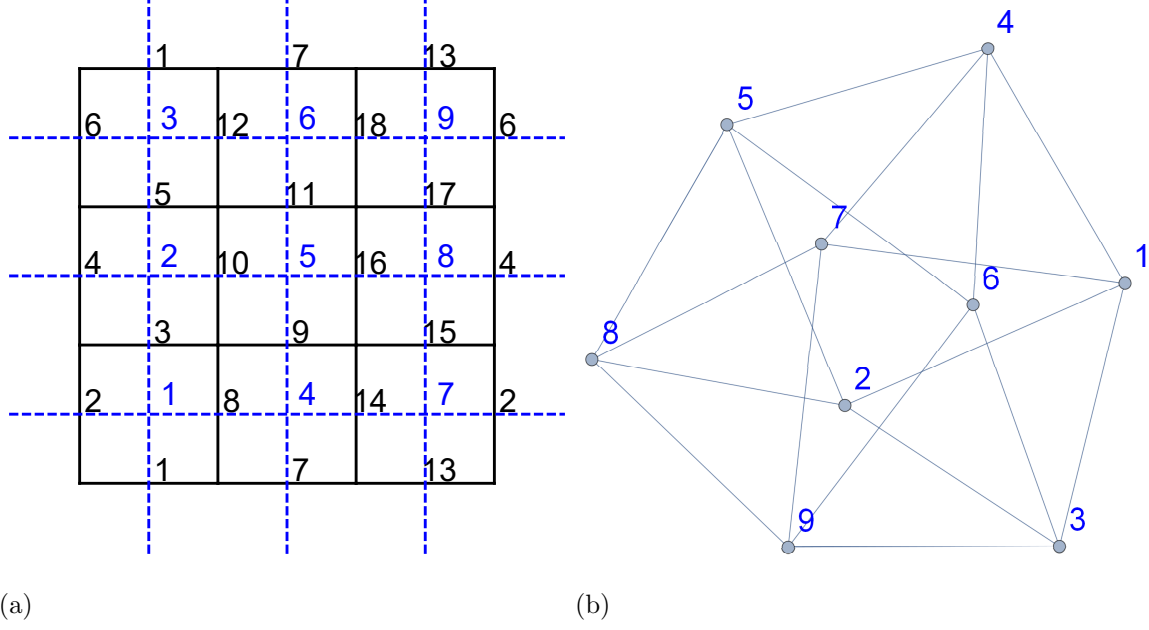
3

FIG. 1. The correspondence between the torus lattice and the graph. (a)The 3*3 torus lattice. The black solid lines are the edges of the lattice, and the blue dotted lines correspond to the edges of the graph. The black numbers are the numbers of the edges of the lattice, and the blue numbers correspond to the vertex numbers of the graph. (b) The graph corresponding to the 3*3 tours lattice.

closed string passes through all N_v plaquettes of the whole lattice, so it is an Hamiltonian cycle. In the configuration of Fig.2(b), two closed strings only pass through part of the N_v plaquettes, so there is no Hamiltonian cycle. If we map the plaquettes to the vertices of a graph, then we have a undirected and unweighted graph of N_v vertices as shown in Fig.1(b). It can be seen that in the deconfined phase, we only need to search for Hamiltonian cycles in the configuration space size of S_0 to determine whether there are Hamiltonian cycles in the lattice of N_v plaquettes. Compared to the original configurations space of size $N_v!$[1], this method greatly reduces search complexity.

III.   THE MAPPING OF A LATTICE AND A GRAPH

We can see that by mapping plaquettes of a lattice to the vertices of the graph we can map the torus lattice to a graph as shown in Fig.1. Two adjacent plaquettes in the lattice are mapped to two adjacent vertices in the graph. The corresponding edge linking the two

plaquettes in the lattice are mapped to the edges linking the two vertices in the graph. Conversely we can also map any graph to a lattice. In this way, the HCP of the graph becomes the HCP of its corresponding lattice. For a lattice mapped by a graph with N_v vertices and N_e edges, in its closed string condensed state there are also $S_0 = O(2^{N_e}/2^{N_v})$ closed string configurations $|\phi_i\rangle$ because all $Z_\square = -1, \forall\square$ in the lattice.

This mapping is very meaningful. As mentioned above, the Hamiltonian cycle search of a lattice can be greatly accelerated by the above Z_2 TQPT. At the same time, the various properties of a graph will inevitably influence the critical parameter g_c of its phase transition, which in turn can reveal the properties of the graph. Here the problem of graph theory and topological quantum phase transitions are neatly linked.

To facilitate discussion, we define several quantities to describe the properties of a graph. N_v is the number of vertices in the graph. N_e is the number of edges in the graph. N_{hc} is the number of Hamiltonian cycles of the graph. $Max(Deg)$ is the maximum degree of the vertices of the graph. $Min(Deg)$ is the minimum degree of the vertices of the graph.

IV. COMPLEXITY OF THE QUANTUM HCP ALGORITHM

The complexity of this quantum algorithm comes from two processes, the first is the process of obtaining the closed string condensed sate, and the second is the process of searching for Hamiltonian cycle states in the closed string condensate.

1) The closed string condenstate can be obtained from the equal weight superposition state through quantum adiabatic evolution[17, 23]. Starting from the equal weight superposition state of all links which is the ground state at $g = +\infty$[8], if we reduce g adiabatically, the state of the system after the critical parameter g_c of the TQPT is the quantum state to be obtained. This process is equivalent to adiabatically evolve the following Hamilton with $\lambda = 0 \rightarrow \lambda_c$. $H_\lambda = \lambda Z + X$, where $\lambda = \frac{1}{g}, \lambda_c = \frac{1}{g_c}$.

According to the adiabatic condition requirements of adiabatic Z_2 quantum simulation, the time scale is $t = O(\sqrt{N_e})$ for a 2-dimensional lattice [23]. So, the time scale is $t = O(\sqrt{N_e})\lambda_c$ for an lattice of an unknown λ_c. According to the symmetric Trotter error formula used in this paper[17], the cumulative error from the start to the phase transition point λ_c can be obtained

$$\varepsilon = O(\frac{1}{N_{ss}^2} N_e^{3/2}(N_v^3 + N_e\lambda_c)\lambda_c^4) \tag{3}$$

5

N_{ss} is the total number of symmetric Trotter substeps.

So, according to the precision requirements of symmetric Trotter decomposition and adiabatic quantum simulation as discussed in the quantum Z_2 simulation method [17, 23], the time complexity required for this process is

$$O_1 = O(\sqrt{\frac{1}{\varepsilon} N_e^{3/2}(N_v^3 + N_e\lambda_c)\lambda_c^4}) = O(\frac{1}{g_c^2}\sqrt{\frac{1}{\varepsilon} N_e^{3/2}(N_v^3 + \frac{N_e}{g_c})}) \tag{4}$$

In a connected undirected graph, the number of edges is not less than the number of its vertices, $N_v \leq N_e \leq N_v(N_v - 1)/2$. ε is precision of the quantum simulation, t is the total time, g_c, λ_c is relatively fixed quantities for a given graph.

2) Searching for Hamiltonian cycles in the closed string condenstates can be done using some quantum search algorithms, which have a complexity of O_2. The closed string condensates is an equal weighted superposition of $S_0 = O(2^{N_e}/2^{N_v})$ components, which contain Hamiltonian cycle states. The probability of obtaining Hamiltonian cycle states by direct measurement is $\frac{N_{hc}}{S_0}$. The relationship between N_{hc} and N_e of some sample graphs is shown in figure 10 (b). However, it is clear that it is possible to develop a better quantum search algorithm for finding Hamiltonian cycle states in the closed string condensates, which is a open question.

So, the total time complexity is $O = O_1 * O_2$. The exponential part of O mainly comes from the second search process.

As mentioned, various properties of a graph may affect the TQPT critical parameters g_c of its corresponding lattice, and thus g_c may in turn reveal the properties of the graph. In the first process, if the value of g_c can reveal the number of Hamiltonian cycles N_{hc}, then it is possible to infer the number of Hamiltonian cycles from the TQPT. Of course, obtaining g_c requires the measurement of H, which requires additional measurement complexity O_M. According to the phase estimation method[17], the measurement complexity can be an order of magnitude as O_1. So, a quantum algorithm of time complexity $O' = O_1 + O_M$ to obtain g_c is found. Because this complexity contains $\lambda_c = \frac{1}{g_c}$, different graphs may have different g_c. Therefore, we need to explore the effect of graph properties (such as N_{hc}) on g_c and the relationship between g_c and N_e to analyze this complexity.

V. THE RELATIONSHIP BETWEEN g_c AND GRAPH

A. Four different graphs for testing the critical parameter g_c

In order to study the effect of graph properties on phase transitions, we first randomly select four graphs shown in Fig.4(a-c) with $N_v = 9, N_e = 18$ to observe the characteristics of phase transition curve of their corresponding lattices. N_{hc} of the four graphs are 0, 10, 30, 48 respectively. The fourth graph is corresponding to the 3×3 torus lattice. All results are listed in Fig.4. We define two g_c: g_c^H represents the extreme point of the second derivative of $\langle H \rangle$ curve and g_c^Z represents the extreme point of the first derivative of the $\langle Z \rangle$ curve. So, $\lambda_c^H = \frac{1}{g_c^H}, \lambda_c^Z = \frac{1}{g_c^Z}$. As can be seen from Fig.4(c-d), the critical parameter g_c of the phase transition increases with N_{hc}. This shows that the properties of the graph will directly affect the the characteristics of the phase transition, which will be investigated in detail below.

B. The relationship between g_c and the number of Hamiltonian cycle N_{hc}

In order to study the effect of N_{hc} on g_c, we prepared two groups of undirected and unweighted connected graphs with $N_v = 9$ vertices. The first group has a total of 1000 samples, each graph has the number of edges $N_e = 18$, and its N_{hc} distribution is shown in the Fig.5(a). The second group of graphs has the number of edges $N_e = 16 - 22$, 200 samples of each N_e, its N_{hc} distribution is shown in the Fig.5(b).

Using the mapping between the plaquettes of the lattice and the vertexs of the graph, each graph is transformed into a corresponding lattice. And the adiabatic quantum simulation method is used to obtain the curve of $\langle H \rangle$ and $\langle Z \rangle$ with g, and then the curve is derived to obtain the critical parameter g_c. It can be seen from the Fig.6 that the mean value of g_c increases steadily with N_{hc} when N_e is fixed. Especially when $N_{hc} = 0$, the mean value of gc decreases significantly. This shows that N_{hc} has a significant effect on g_c. Using this effect can help determine the number of N_{hc} of a graph through TQPT without searching the path of the graph. The number of quantum gates required to complete the TQPT is O_1. And $\frac{1}{g_c}$ may increase linearly with N_e as discussed below. Also $N_v \leq N_e \leq N_v(N_v - 1)/2$, it means that HCP on quantum computer has the possibility of P time complexity algorithm.

7

C. The relationship between g_c and the number of edge N_e

In order to study the effect of N_e on g_c, we use the second group of graphs with same N_v but different N_e. As can be seen from the Fig.7, the average value of g_c decreases steadily with N_e when N_v is fixed. On average, when N_v is fixed the connectivity between vertices of a graph is proportional to N_e. From the perspective of a lattice, this means that the strength of the connection between plaquettes is proportional to N_e. Therefore, the larger the N_e, the lower the critical parameter g_c of the phase transition. In particular, the average value of $\lambda_c = \frac{1}{g_c}$ increase linearly with N_e when N_v is fixed, which support the P complexity of above algorithm.

D. The relationship between g_c and the degree of vertices

In order to study the effect of degree of a graph on g_c, we use this two groups of graphs. As can be seen from the Fig.8, the average value of g_c decreases with $Max(Deg)$ and increases with $Min(Deg)$ when N_e, N_v is fixed. $Max(Deg)$ and $Min(Deg)$ reflects the equilibrium of vertex connection. On average, when N_v and N_e is fixed, the larger $Max(Deg)$, the smaller $(Min(Deg))$. So the data of Fig.8(a,c) and Fig.8(b,d) echo each other. And on average, when N_v and N_e is fixed, the larger $Max(Deg)$, the smaller N_{hc}. So the data of Fig.8 and Fig.6 are also consistent with each other.

E. Fit analysis

In the above part, combined with the numerical simulation results, we make a qualitative analysis of the changes of g_c with various properties of the graph, and the results reveal that the graph properties have an obvious effect on g_c. Next, we will conduct quantitative fitting analysis on two of above key results.

1) Fitting analysis of g_c^H mean value curve with N_{hc}. In turn, g_c can be used to reveal the number of Hamiltonian cycles in the graph by means of the influence of N_{hc} on g_c, which is a core of the above quantum algorithm. Therefore, it is very important to find the quantitative relationship between g_c and N_{hc}. According to the shape of the curve, empirically we find

that the following formula can get a good fitting result

$$g_c^H = A\sqrt{N_{hc}} + B \tag{5}$$

We use this formula to fit the two groups of samples, and the results are shown in Fig.9. It can be seen that a very good fitting effect is obtained. g_c^H and N_{hc} show a linear growth relationship. Of course, this is the result of the empirical fitting of the curve shape, and the theoretical reasons need to be solved.

2) Fitting analysis of $\lambda_c = \frac{1}{g_c}$ mean value curve with N_e. From the qualitative analysis above, it can be seen that λ_c^H and N_e present a linear relationship, and a very good result is obtained by linear fitting as shown in Fig.10. The fitting result is $\lambda_c^H = 0.1513 * N_e + 0.007536$. Of course, due to the limitation of computing power, the number of edges in our simulated graphs is still relatively small, so the linear relationship needs more graphs to verify.

VI.   QUANTUM SIMULATION METHOD

The quantum circuits and quantum adiabatic simulation scheme is referenced to our previous studies[17] . In terms of software, we use the QuEST GPU quantum simulator[24]. In terms of computing hardware, we use the latest and most powerful Nvidia GPU: Tesla V100-SXM2-32GB.

We use the symmetric Trotter decomposition to decompose the Hamilton, which is more efficient than the origin Trotter[25, 26], The error of the adiabatic simulation step can be referred to our previous studies [17].

$$
\begin{aligned}
\varepsilon_s(t, n, g) &= |e^{-i(A+B)t} - (e^{-iA\frac{t}{2n}} e^{-iB\frac{t}{n}} e^{-iA\frac{t}{2n}})^n| \\
&= |e^{-i(A+B)t} - e^{-iA\frac{t}{2n}} (e^{-iB\frac{t}{n}} e^{-iA\frac{t}{n}})^{n-1} e^{-iB\frac{t}{n}} e^{-iA\frac{t}{2n}}| \\
&\leqslant (\frac{1}{12} g^2 N_v * 16 + \frac{1}{24} g N_e * n_p^2) \frac{t^3}{n^2}
\end{aligned}
\tag{6}
$$

t is total time of the step , n is number of symmetric Trotter substeps. For this article d=2 lattice: $N_v = 9, 16 \leqslant N_e \leqslant 22, n_p = 2$. n_p is the number of vertices adjacent to each edge or is the number of plaquettes adjacent to each link.

The starting ground state $|\psi_0\rangle$ at $g = 0$ is $Z_\square = -1, \forall \square$. In the $M * N$ torus lattice, this starting ground state $|\psi_0\rangle = \sum_{i=1}^{S_0} |\phi_i\rangle$ contains $S_0 = 2^{N_e}/(2^{N_v} - 1), N_e = 2MN, N_v = MN$ superposed base vector components $|\phi_i\rangle$. For a lattice mapped by a graph with N_v vertices

and N_e edges, in its closed string condenstate there are also $S_0 = O(2^{N_e}/2^{N_v})$ closed string configurations $|\phi_i\rangle$

We first increase g from 0 to 1 adiabaticly by adiabatic step $g_s = 0.001, t_s = 0.1, n = 100$. t_s, n are the time and the number of symmetric Trotter substeps of each step respectively. The total cumulative error is $\varepsilon_{all} = \sum_{g=g_s}^{1} \varepsilon_s(t, n, g)$. So, ε_{all} is less than 0.135% for the graphs in this article.

VII. CONCLUSION AND DISCUSSION

In Conclusion, using the condensed close string characteristics of the Z_2 TQPT, we develop a quantum model of graph problem by transforming a graph to a lattice. And then a $O(\frac{1}{g_c^2}\sqrt{\frac{1}{\varepsilon}N_e^{3/2}(N_v^3 + \frac{N_e}{g_c})})$ adiabatic quatum algorithm to obtain the closed string condensate of its corresponding lattice can be designed. In this quantum model, we also find that the Hamiltonian cycle number N_{hc} of a graph has a significant effect on the TQPT critical parameter g_c of its corresponding lattice, thus giving a novel quantum algorithm for HCP, which open up the new possibility of HCP on quantum computer. In view of the important position of graph theory in computer science and mathematics, this quantum graph model will have a very beneficial impact in many fields. For example, deep learning represented by deep neural networks are being integrated with graphical models[11–13]. The model's solution to graph problems is also conducive to the development of these fields. In addition, the model connects the two hot-spot areas of graph problems and TQPT. It is believed that the mutual turbulence of these two areas will produce rich new results.

VIII. ACKNOWLEDGE

[1] M. R. Garey and D. S. Johnson, *Computers and Intractability; A Guide to the Theory of NP-Completeness* (W. H. Freeman & Co., USA, 1990).

[2] J. van Leeuwen, ed., *Handbook of Theoretical Computer Science (Vol. B): Formal Models and Semantics* (MIT Press, Cambridge, MA, USA, 1991).

[3] R. Bellman, "Dynamic programming treatment of the travelling salesman problem," J. ACM **9**, 61 (1962).

[4] A. Björklund, "Determinant sums for undirected hamiltonicity," in *2010 IEEE 51st Annual Symposium on Foundations of Computer Science* (2010) pp. 173–182.

[5] P. W. Shor, "Algorithms for quantum computation: discrete logarithms and factoring," in *Proceedings 35th Annual Symposium on Foundations of Computer Science* (1994) pp. 124–134.

[6] Anuradha Mahasinghe, Richard Hua, Michael J. Dinneen, and Rajni Goyal, "Solving the hamiltonian cycle problem using a quantum computer," in *Proceedings of the Australasian Computer Science Week Multiconference*, ACSW 2019 (Association for Computing Machinery, New York, NY, USA, 2019).

[7] J. B. Kogut, "An introduction to lattice gauge theory and spin systems," Rev. Mod. Phys. **51**, 659 (1979).

[8] S. Sachdev, "Topological order, emergent gauge fields, and fermi surface reconstruction," Rep. Prog. Phys. **82**, 014001 (2018).

[9] M. A. Levin and X. G. Wen, "String-net condensation: A physical mechanism for topological phases," Phys. Rev. B **71**, 045110 (2005).

[10] X. G. Wen, "An introduction to quantum order, string-net condensation, and emergence of light and fermions," Ann. Phys. **316**, 1 (2005).

[11] M. J. Johnson, D. Duvenaud, A. B. Wiltschko, S. R. Datta, and R. P. Adams, "Composing graphical models with neural networks for structured representations and fast inference," arXiv e-prints , arXiv:1603.06277 (2016).

[12] H. Wang and D. Yeung, "Towards bayesian deep learning: A framework and some existing methods," IEEE Trans. Knowl. Data Eng. **28**, 3395 (2016).

[13] M. H. Amin, E. Andriyash, J. Rolfe, B. Kulchytskyy, and R. Melko, "Quantum boltzmann machine," Phys. Rev. X **8**, 021050 (2018).

[14] J. Biamonte, P. Wittek, N. Pancotti, P. Rebentrost, N. Wiebe, and S. Lloyd, "Quantum machine learning," Nature **549**, 195–202 (2017).

[15] S. Lloyd, "Universal quantum simulators," Science **273**, 1073 (1996).

[16] E. Zohar, A. Farace, B. Reznik, and J. I. Cirac, "Digital quantum simulation of z(2) lattice gauge theories with dynamical fermionic matter," Phys. Rev. Lett. **118**, 5 (2017).

[17] X. Cui, Y. Shi, and J. C. Yang, "Circuit-based digital adiabatic quantum simulation and pseudoquantum simulation as new approaches to lattice gauge theory," J. High Energy Phys **2020**, 160 (2020).

[18] H. Lamm, S. Lawrence, and Y. Yamauchi (NuQS Collaboration), "General methods for digital quantum simulation of gauge theories," Phys. Rev. D **100**, 034518 (2019).

[19] R. Barends, A. Shabani, L. Lamata, J. Kelly, A. Mezzacapo, U. L. Heras, R. Babbush, A. G. Fowler, B. Campbell, Y. Chen, Z. Chen, B. Chiaro, A. Dunsworth, E. Jeffrey, E. Lucero, A. Megrant, J. Y. Mutus, M. Neeley, C. Neill, P. J. J. O'Malley, C. Quintana, P. Roushan, D. Sank, A. Vainsencher, J. Wenner, T. C. White, E. Solano, H. Neven, and J. M. Martinis, "Digitized adiabatic quantum computing with a superconducting circuit," Nature **534**, 222 (2016).

[20] Y. Shi and Y. S. Wu, "Perturbative formulation and nonadiabatic corrections in adiabatic quantum-computing schemes," Phys. Rev. A **69**, 024301 (2004).

[21] S. Bachmann, W. De Roeck, and M. Fraas, "Adiabatic theorem for quantum spin systems," Phys. Rev. Lett. **119**, 060201 (2017).

[22] F. J. Wegner, "Duality in generalized ising models and phase transitions without local order parameters," J. Math. Phys. **12**, 2259 (1971).

[23] A. Hamma and D. A. Lidar, "Adiabatic preparation of topological order," Phys. Rev. Lett. **100**, 4 (2008).

[24] T. Jones, A. Brown, I. Bush, and S. C. Benjamin, "QuEST and High Performance Simulation of Quantum Computers," Sci. Rep. **9**, 10736 (2019).

[25] H. F. Trotter, "On the product of semi-groups of operators," Proc. Am. Math. Soc. **10**, 545 (1959).

[26] A. M. Childs, Y. Su, M. C. Tran, N. Wiebe, and S. Zhu, "A Theory of Trotter Error," arXiv e-prints , arXiv:1912.08854 (2019).
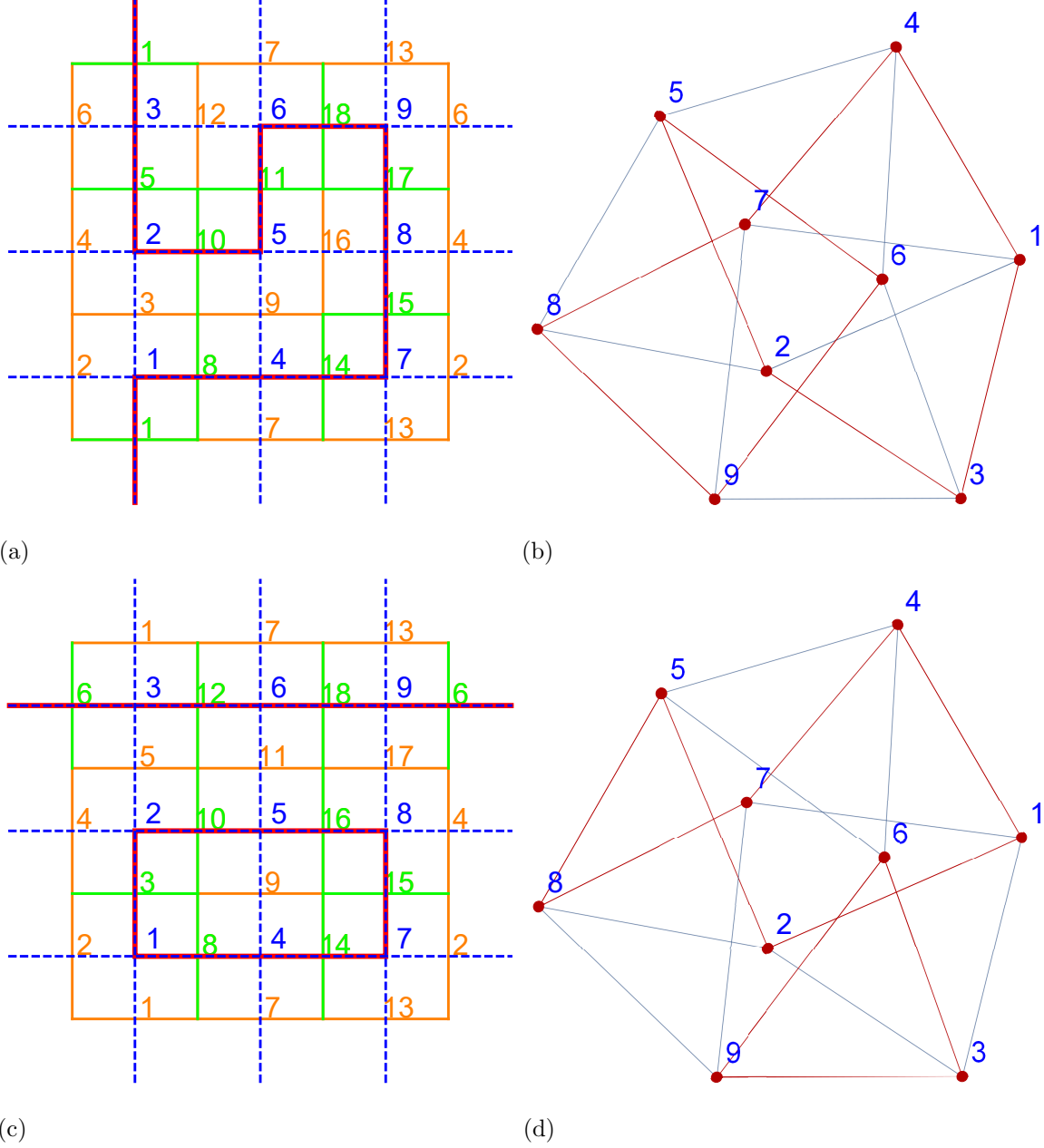
(a)

(b)

(c)

(d)

FIG. 2. The correspondence between the closed string of the torus lattice and the cycle of the graph. (a) At g = 0, a closed string configuration of the Z_2 ground state. There is only one closed string (shown in the red path). The green edge is in the $|0\rangle$ state, and the orange edge is in the $|1\rangle$ state. (b) The hamiltonian cycle of the graph(red path) cor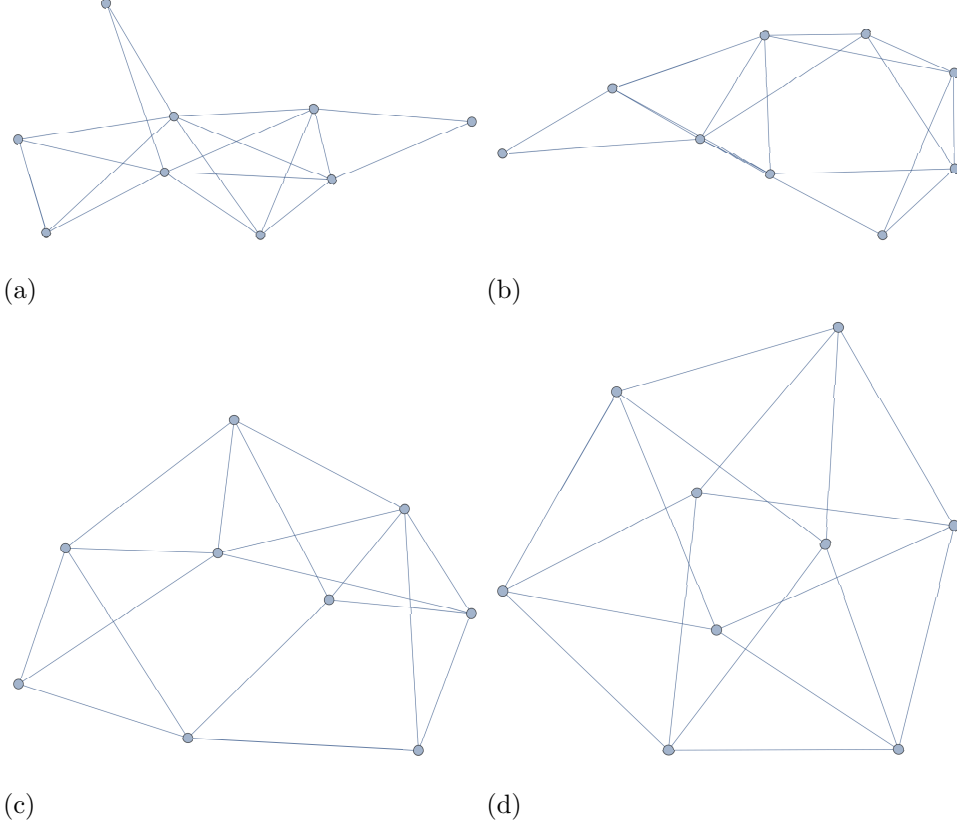responding to the closed string in the tours lattice. (c) At g = 0, a closed string configuration of the Z_2 ground state with two closed string (shown in the red path). The green edge is in the $|0\rangle$ state, and the orange edge is in the $|1\rangle$ state. (d) The cycle of the graph(red path) corresponding to the closed string in the tours lattice.

13

FIG. 3. Three different graphs for testing the critical parameter g_c of Z_2 TQPT. (a) $G_1 : N_v = 9, N_e = 18, N_{hc} = 0$. (b) $G_2 : N_v = 9, N_e = 18, N_{hc} = 10$. (c) $G_3 : N_v = 9, N_e = 18, N_{hc} = 30$. (d) G_4: the graph of the 3*3 torus lattice, $N_v = 9, N_e = 18, N_{hc} = 48$.
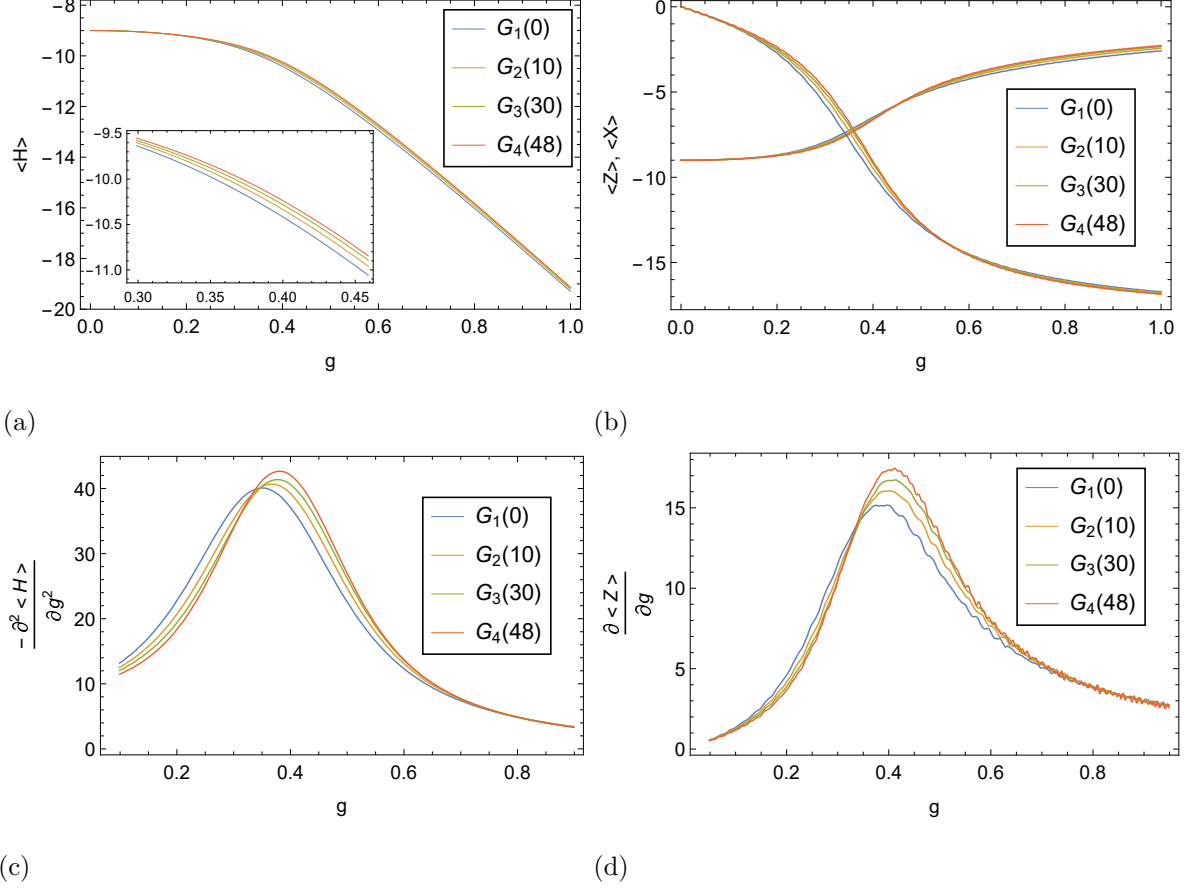
FIG. 4. The critical parameter g_c for three testing graphs . (a-b) The QPT curves(H, Z, X) for three testing graphs. (c) The second derivative curves of H for three testing graphs, which can be used to determine critical parameter g_c^H for three testing graphs. (d) The first derivative curves of Z for three testing graphs, which can be used to determine critical parameter g_c^Z for three testing graphs.
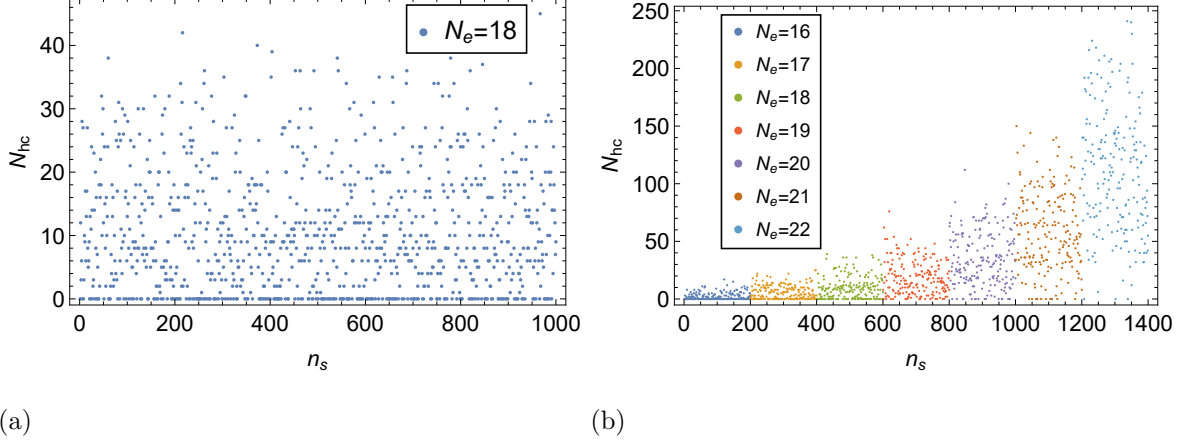
(a)   (b)

FIG. 5. Distribution of the N_{hc} of all samples. n_s is the number of the samples. (a) The number of edges is $N_e = 18$ per sample, 1000 samples in total. (b) The number of edges is $N_e = 16 - 22$, 1400 samples in total, 200 samples per N_e.
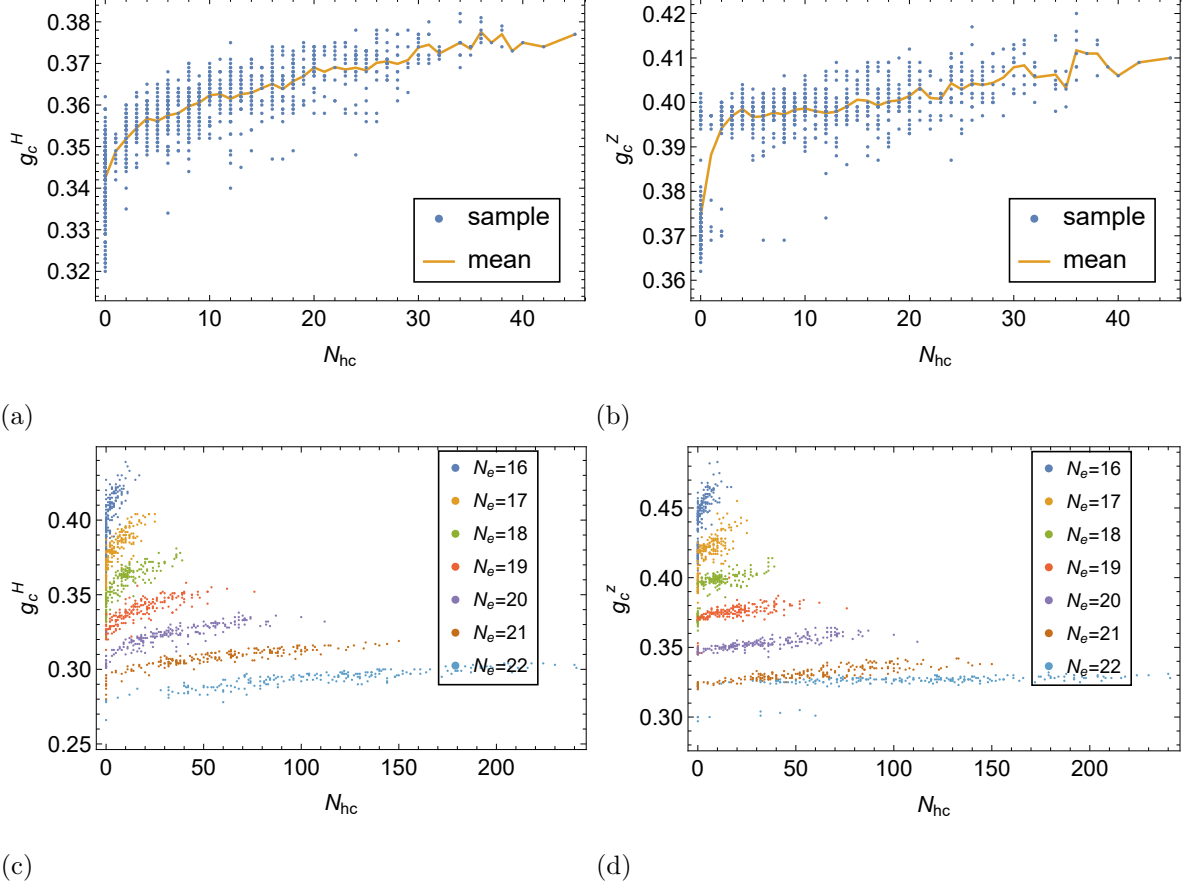
(a)

(b)

(c)

(d)

FIG. 6. Change of critical parameter g_c with the number of Hamiltonian cycles N_{hc}. (a) Critical parameter g_c^H change with the number of Hamiltonian cycles N_{hc} in the $N_e = 18$ samples. (b) Critical parameter g_c^Z change with the number of Hamiltonian cycles N_{hc} in the $N_e = 18$ samples. (c) Critical parameter g_c^H change with the number of Hamiltonian cycles N_{hc} in the $N_e = 16 - 22$ samples. (d) Critical parameter g_c^Z change with the number of Hamiltonian cycles N_{hc} in the $N_e = 16 - 22$ samples.
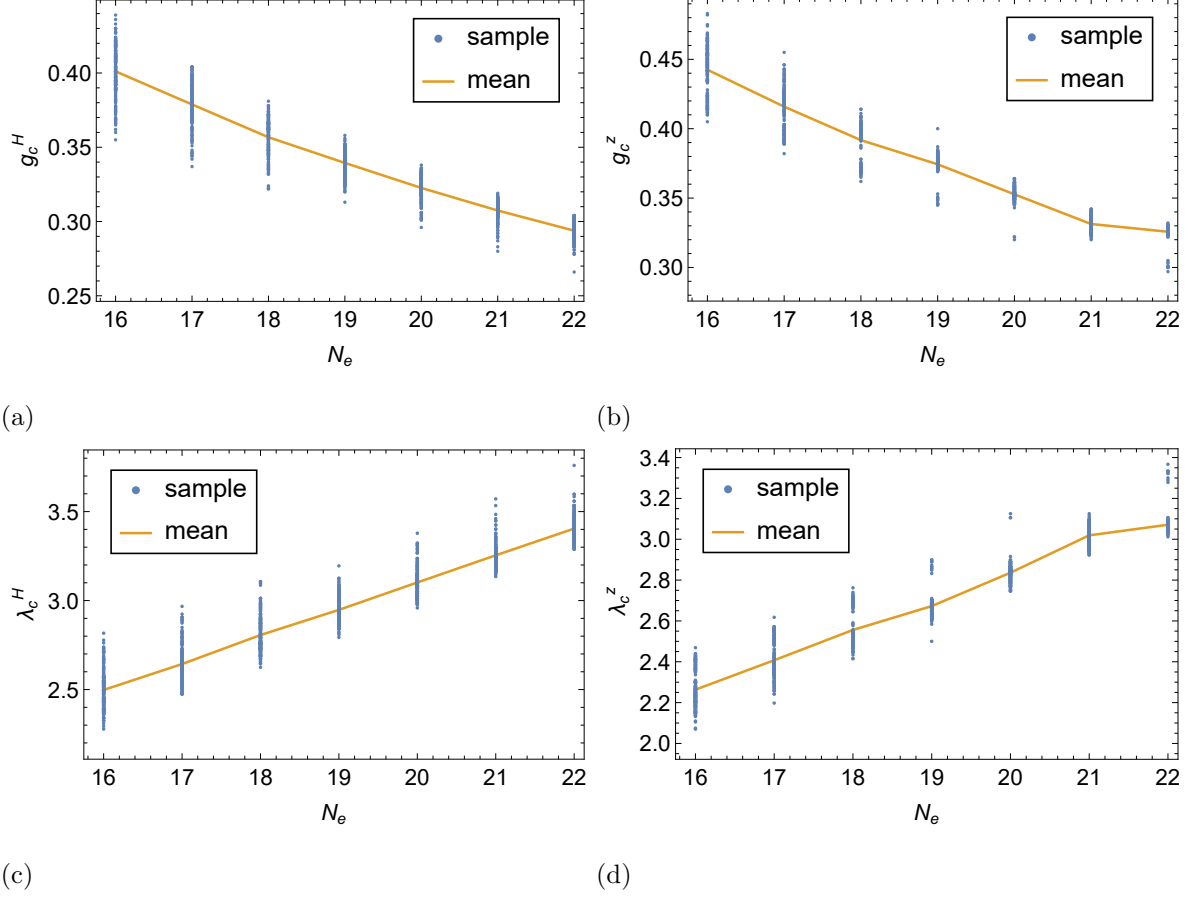
(a)

(b)

(c)

(d)

FIG. 7. Change of critical parameter g_c with the number of edges N_e. (a) Critical parameter g_c^H change with the number of edges N_e in the $N_e = 16 - 22$ samples. (b) Critical parameter g_c^Z change with the number of edges N_e in the $N_e = 16 - 22$ samples.(c) Critical parameter λ_c^H change with the number of edges N_e in the $N_e = 16 - 22$ samples. (d) Critical parameter λ_c^Z change with the number of edges N_e in the $N_e = 16 - 22$ samples.
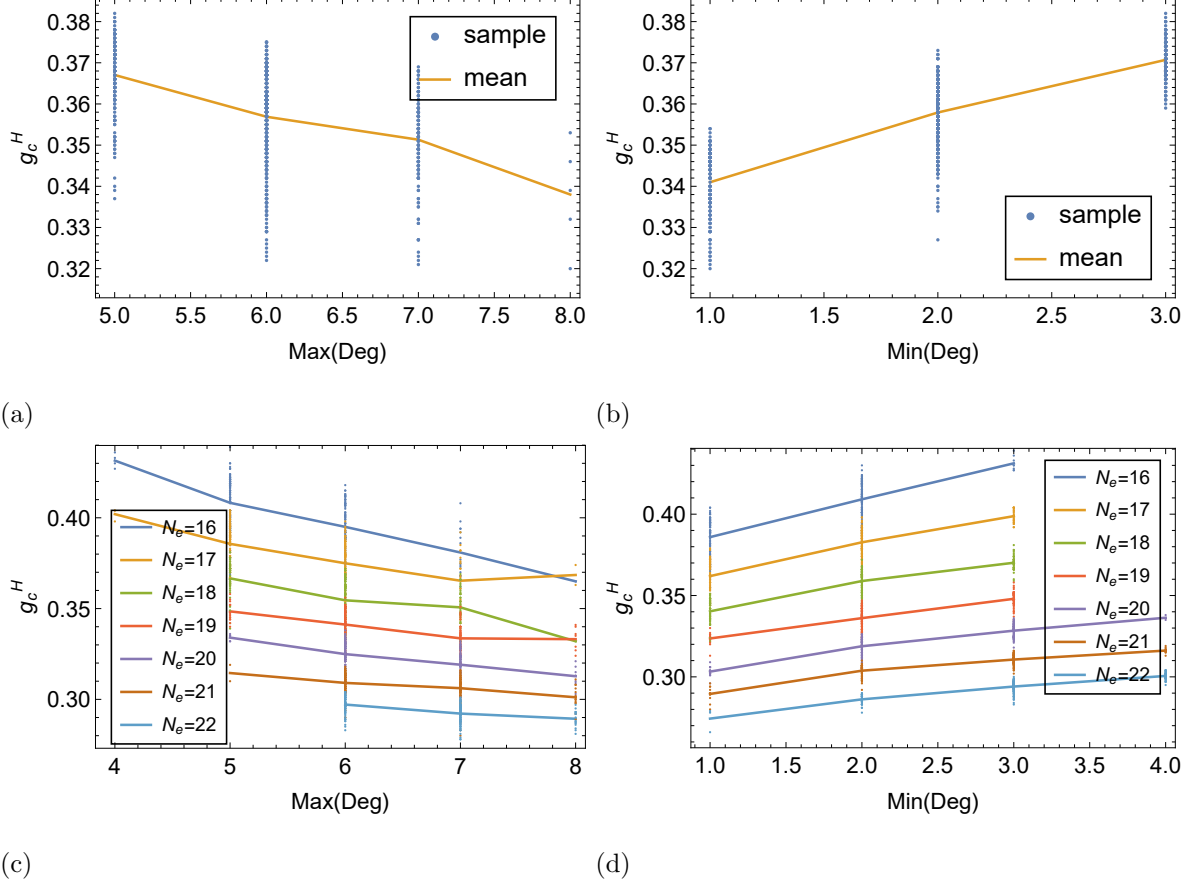
FIG. 8. Change of critical parameter g_c with the degree of vertexs. (a) Critical parameter g_c^H change with the max degree $Max(Deg)$ of vertexs in the $N_e = 18$ samples. (b) Critical parameter g_c^H change with the min degree $Min(Deg)$ of vertexs in the $N_e = 18$ samples. (c) Critical parameter g_c^H change with the max degree $Max(Deg)$ of vertexs in the $N_e = 16 - 22$ samples. (d) Critical parameter g_c^H change with the min degree $Min(Deg)$ of vertexs in the $N_e = 16 - 22$ samples.
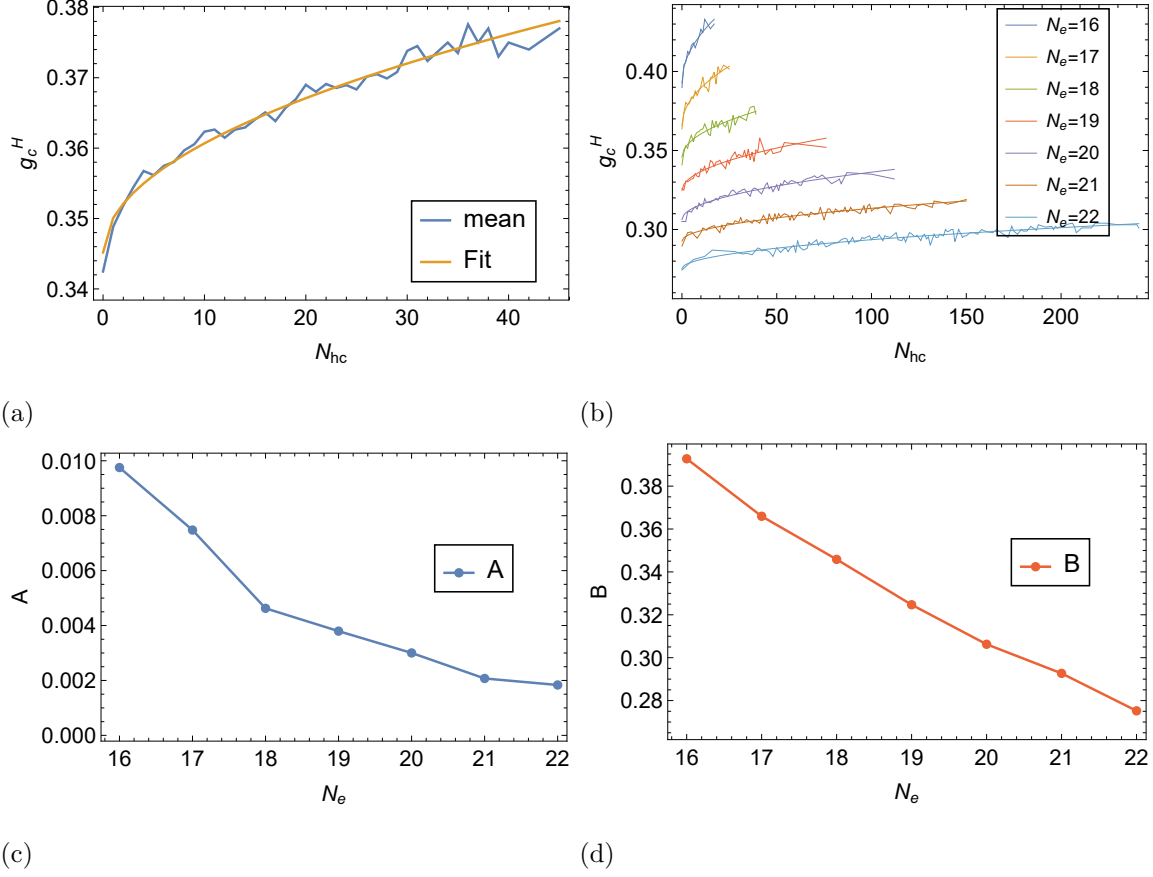
(a)

(b)

(c)

(d)

FIG. 9. Fitting analysis of Critical parameters g_c^H mean value with N_{hc} curve , the fitting function using $g_c^H = A\sqrt{N_{hc}} + B$. (a) In the $N_e = 18$ samples, the fitting curve of the mean value of the critical parameters g_c^H with the number of Hamiltonian cycles N_{hc}, the fitting result is $A = 0.0049005, B = 0.345178$. (b) In the $N_e = 16 \sim 22$ samples, the fitting curve of the mean value of the critical parameter g_c^H with the number of Hamiltonian cycles N_{hc}. (c) The curve of the fitting parameter A in (b) with the number of edges N_e. The curve of the fitting parameter B in (d) with the number of edges N_e.
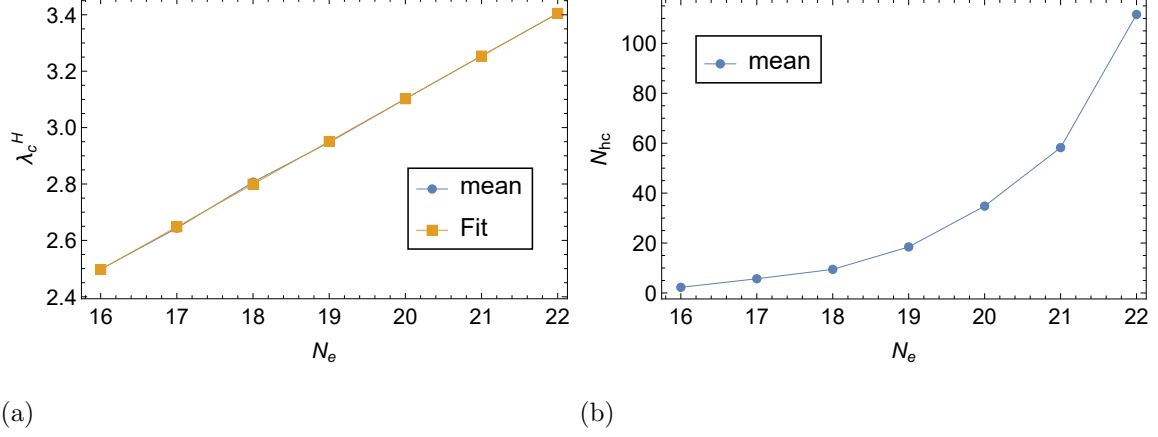
(a)   (b)

FIG. 10. Linear fitting analysis of the mean value of critical parameter λ_c^H with N_e. (a) The fitting curve of the mean value of critical parameter λ_c^H with the number of edges N_e in the $N_e = 16 \sim 22$ samples. The fitting result is $\lambda_c^H = 0.1513 * N_e + 0.07536$. (b) The curve of the mean value of N_{hc} with the number of edges N_e in the $N_e = 16 \sim 22$ samples.